

Supplementary Information:

Chemically Selective Raising and Rolling of Oil-Droplet Underwater: An Equipment-Free Chemical Sensing Method

Experimental section

Materials

Branched polyethyleneimine (BPEI; molecular weight is 25,000 Da), dipentaerythritol pentaacrylate (5Acl; molecular weight is 524.21 g mol⁻¹), N-Phenylethylenediamine (PEDA), 2-carboxyethyl acrylate (CEA), pentyl amine (PA), sulphanilamide, p-terephthalaldehyde (TPA), 2-amino-2-methyl-1-propanol (AMP), hydrazine were purchased from Sigma-Aldrich, India. Dichloroethane (DCE) was acquired from Loba Chemie Pvt. Ltd., India. Ethanol was purchased from TEDIA Company (USA). sodium nitrite, sodium nitrate, sodium chloride, sodium bromide, sodium sulphate, sodium carbonate, sodium phosphate, and hydrochloric acid were procured from Merck Specialities Pvt. Ltd, Mumbai, India. Mili-Q grade water was used for all experiments.

Characterization:

The contact angles and roll-off angles were measured at five different positions for each sample using a KRUSS Drop Shape Analyzer-DSA25 instrument at ambient temperature. The surface topography of the fabricated multilayer was visualized using a field emission electron microscope (FESEM, Sigma Carl Zeiss). All samples were first subjected to gold sputtering to form a thin gold layer prior to imaging. Attenuated total reflection Fourier transform infrared (ATR-FTIR) spectra were recorded using PerkinElmer UATR Two at ambient conditions. Digital photographs were captured using a Canon powershot SX540HS digital camera.

Fabrication of dual-reactive multilayer coatings:

Two ethanol solutions of 5Acl (132.5 mg mL⁻¹) and BPEI (50 mg mL⁻¹) were prepared and mixed to obtain a solution with a 1:10 ratio of BPEI:5Acl. After 15 minutes of mixing, the solution resulted a turbid solution due to formation of the polymeric nanocomplex. The

multilayer coatings were prepared through a layer-by-layer (LbL) deposition process of BPEI and polymeric nanocomplex. First, a glass substrate (7.5 cm × 1.0 cm) was placed in the BPEI solution for 10 seconds. Next, the substrate was removed and washed with an ethanol bath for 10 seconds, followed by a second ethanol bath for another 10 seconds to remove the unabsorbed or loosely absorbed polymers. Subsequently, the substrate was dipped in a dispersion of growing chemically reactive nanocomplex solution in ethanol for 10 seconds and then washed using two ethanol baths. This cycle was repeated 20 times to fabricate a porous polymeric coating of 20 bilayers.

Mono- and dual-functionalization of multilayer coatings:

The multilayers of chemically reactive nanocomplexes comprised of residual acrylate and primary amine groups provide an opportunity for post-modification with rationally selected small molecules via a 1,4-conjugate addition reaction at ambient conditions. First, to achieve the nitrite ion responsive interface, the residual acrylates of the multilayers were post-modified with hydrophobic N-penylethylenediamine (PEDA, 25 $\mu\text{L}/\text{mL}$ in ethanol), by exposing the multilayer coatings in the PEDA solutions for 12 hours at ambient conditions. After PEDA modification, the multilayers were washed with ethanol and dried in air. For dual functionalization, mono (PEDA)-functionalized multilayers were further treated with an ethanol solution consisting of a hydrophilic acrylate, 2-carboxyethyl acrylate (CEA, 25 $\mu\text{L}/\text{mL}$), overnight at ambient conditions, and next washed with ethanol and air dried.

To achieve hydrazine-responsive mono-functionalized coating, the multilayer coating were treated with p-terephthalaldehyde (TPA, 25 $\mu\text{L}/\text{mL}$ in ethanol) for 6 hours at ambient conditions and then washed with ethanol and air dried. For dual functionalization, the TPA-functionalized multilayers were subsequently treated with an ethanol solution of a hydrophilic amine, 2-amino-2-methyl-1-propanol (AMP, 25 $\mu\text{L}/\text{mL}$), overnight at ambient conditions, and next washed with ethanol and air dried.

Nitrite ion sensing with mono- and dual-functionalized multilayer coating:

For sensing experiments, a 1 mM stock solution of nitrite ions in DI water was prepared, and subsequently, different solutions of varying concentrations of nitrite ions in DI water were prepared by diluting the stock solution. The solutions of nitrite ions were then mixed with 0.5 % sulfanilamide solution (prepared in 0.1N HCl) in a 1:1 ratio. The mono (PEDA) and dual (PEDA/CEA)-functionalized multilayer coatings were treated separately with the as-prepared

solutions containing varying concentrations of nitrite ions for 15 minutes. After the successful Griess reaction, the modified coatings were washed thoroughly with DI water to remove the unreacted reactants and then air dried. Next, the contact angle goniometer instrument was used to characterize the increase in the underwater oil wettability in the mono-functioned coating and the decrease in the underwater oil adhesion in the dual-functionalized coating.

Hydrazine sensing with mono- and dual-functionalized multilayer coating:

For hydrazine sensing experiments, different solutions containing different hydrazine concentrations were prepared in DI water by diluting a stock solution. The mono (TPA) and dual (TPA/AMP)-functionalized multilayer coatings were treated separately with the hydrazine solution for 30 minutes. After the conversion of the residual aldehydes on the mono- and dual-functionalized coating to hydrazones, the coatings were washed thoroughly with DI water to remove the unreacted hydrazines and then air dried. Next, the contact angle goniometer instrument was used to characterize the increase in the underwater oil wettability in the mono-functioned coating and the decrease in the underwater oil adhesion in the dual-functionalized coating.

To demonstrate the reusability of the hydrazine-responsive coatings, the hydrazine (120 μ M) modified coating was exposed to an acidic solution (pH 3) to hydrolyze the imine bonds in the coating. The coating was then post-modified with TPA and subsequently treated with hydrazine (120 μ M) following the above-mentioned procedures. The hydrazine exposure resulted in an increase in the underwater oil contact angle. This process was repeated for several cycles to demonstrate the reusability of the coating.

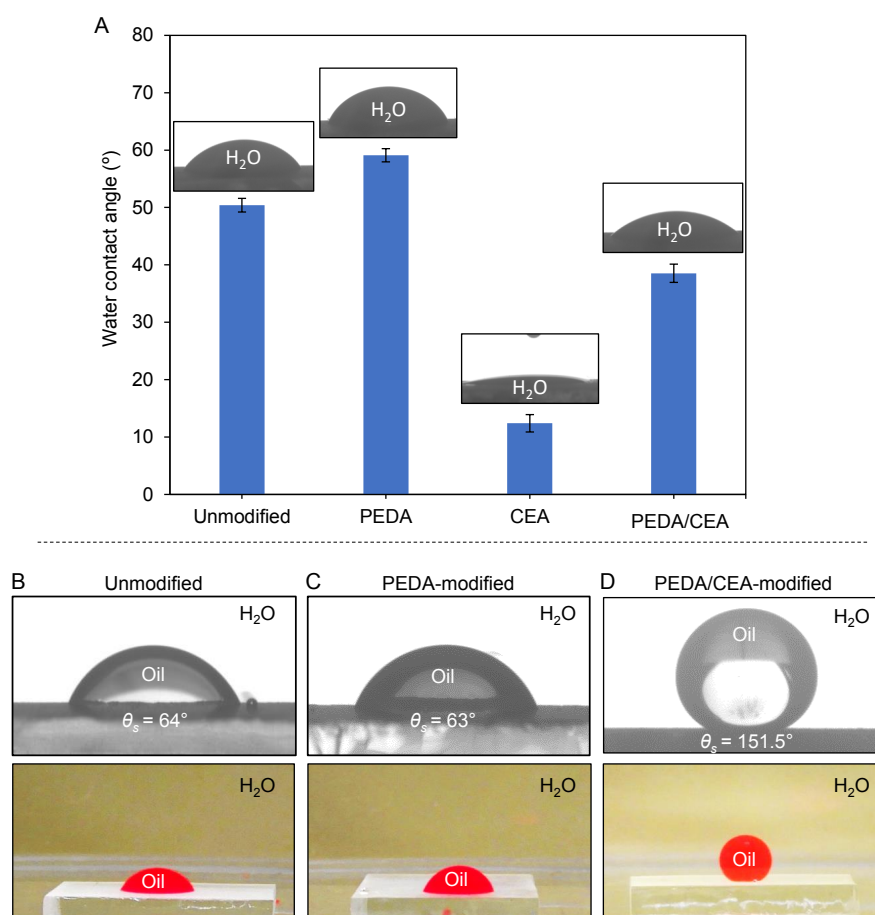


Fig. S1. A) Effect of different mono- and dual-functionalizations on the static water contact angle of 5 μL water droplets on the modified coating. B-D) Contact angle goniometer and digital images showing underwater oil wettability of 5 μL oil droplets (DCE, red dyed) on unmodified, mono (PEDA)-functionalization and dual (PEDA/CEA)-functionalization multilayer coating.

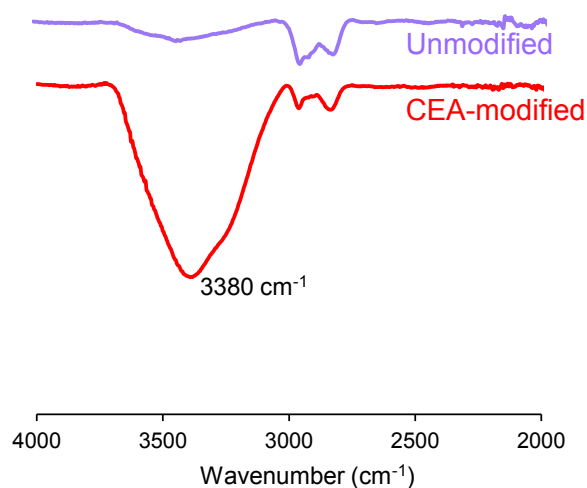


Fig. S2. Attenuated total reflection-Fourier transform infrared (ATR-FTIR) spectra showing the appearance of a broad OH stretching band in the multilayer coatings after modification with CEA.

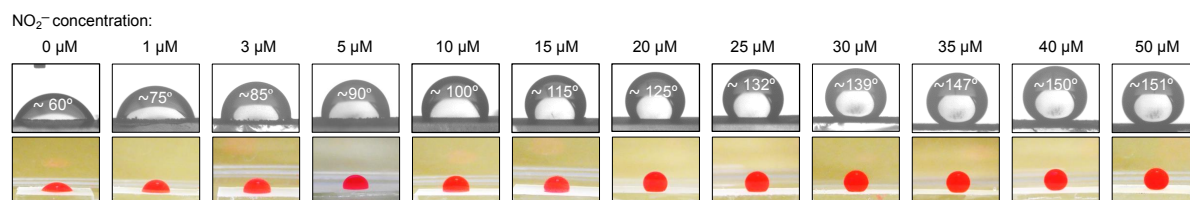


Fig. S3. Contact angle goniometer images and photographs show the effect of the concentration of nitrite ions (during Griess modification) on the static contact angle of oil droplets on PEDA-modified multilayer coatings.

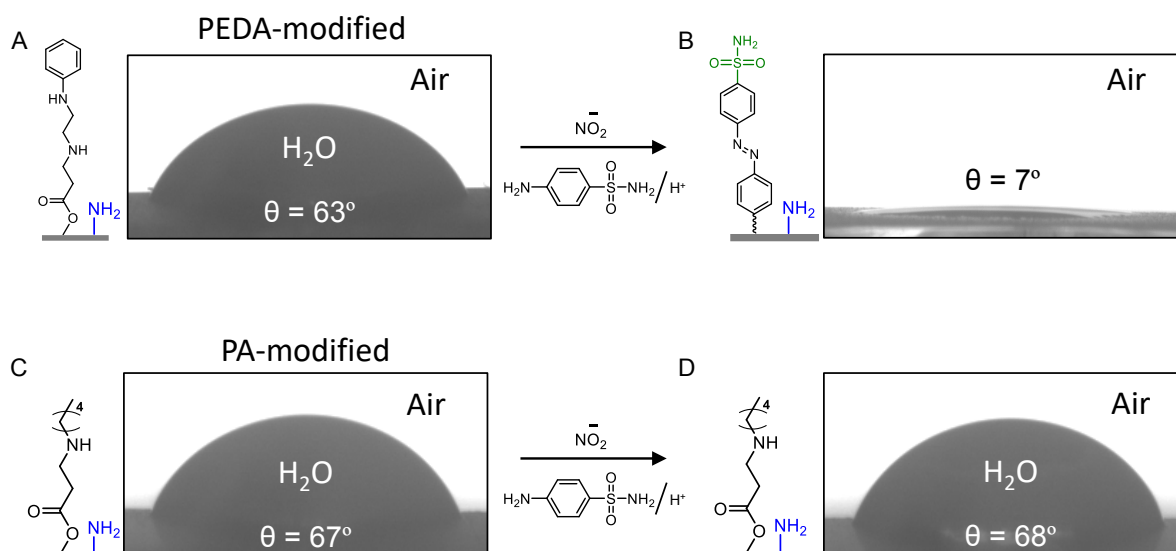


Fig. S4. A-B) Chemical reaction shows the conversion of phenyl moiety in the PEDA-modified coating into hydrophilic sulphonamide moiety through the modified Griess reaction, which is indicated by the depletion of water contact angle. C-D) Chemical functionalities in the PA-modified coating that cannot show conversion through modified Griess reaction and the contact angle goniometer images depict the unaltered water wettability. Water droplet volume is 5 μL .

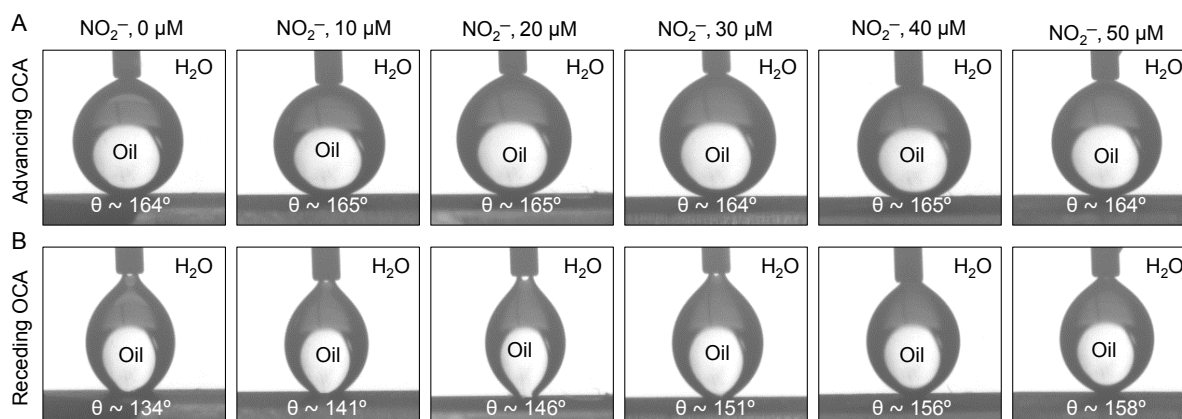


Fig. S5. A-B) Contact angle goniometer images showing (A) advancing and (B) receding oil contact angle on PEA/CEA-modified coating after modified Griess reaction in the presence of the specified nitrite ion concentration. Oil droplet volume was 5 μL .

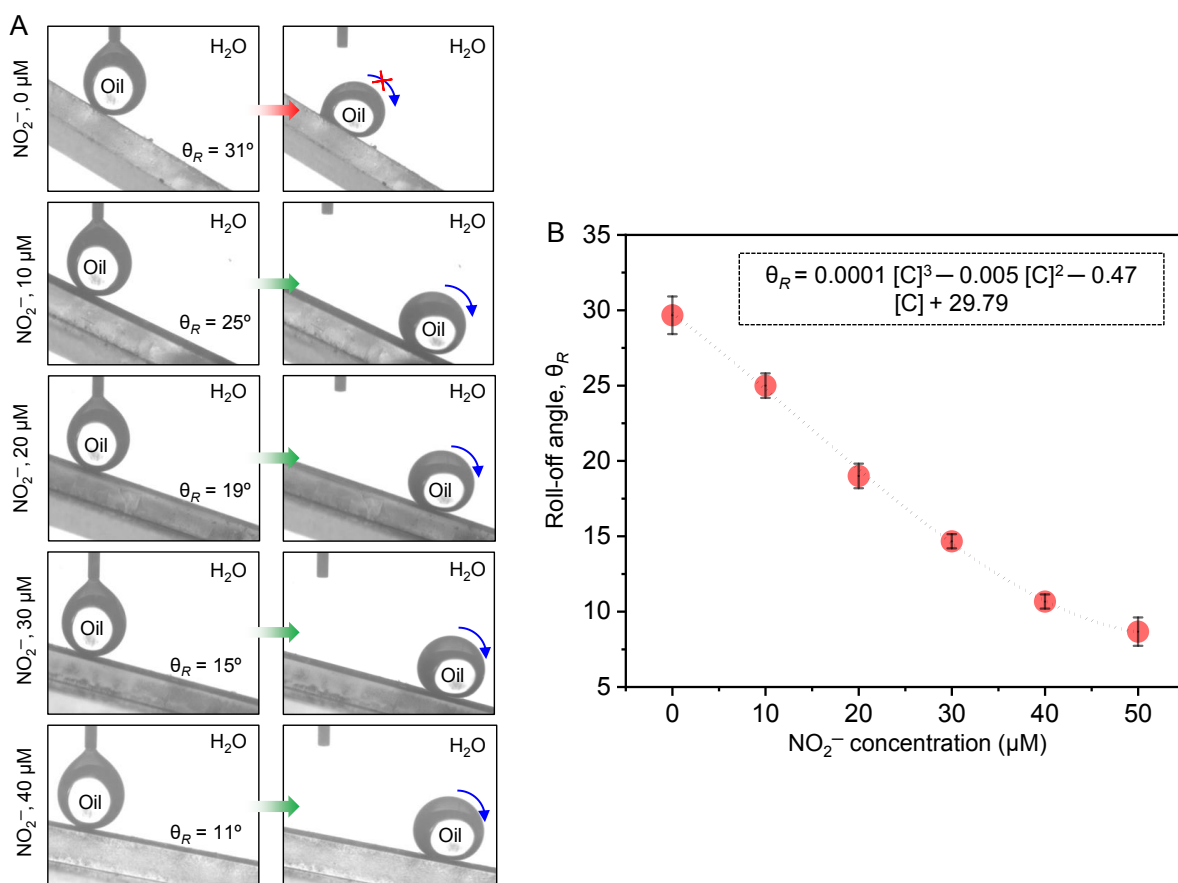


Fig. S6. A) Photographs of the mobility of oil droplets on PEDA/CEA-modified coating after Griess reaction as a function of nitrite ion concentration $[C]$, at a minimum tilting angle where the oil droplets started rolling off. The volume of the beaded oil droplets was $5 \mu\text{L}$. B) Curve shows the roll-off angle (θ_R) of oil droplets as a function of nitrite ion concentration $[C]$.

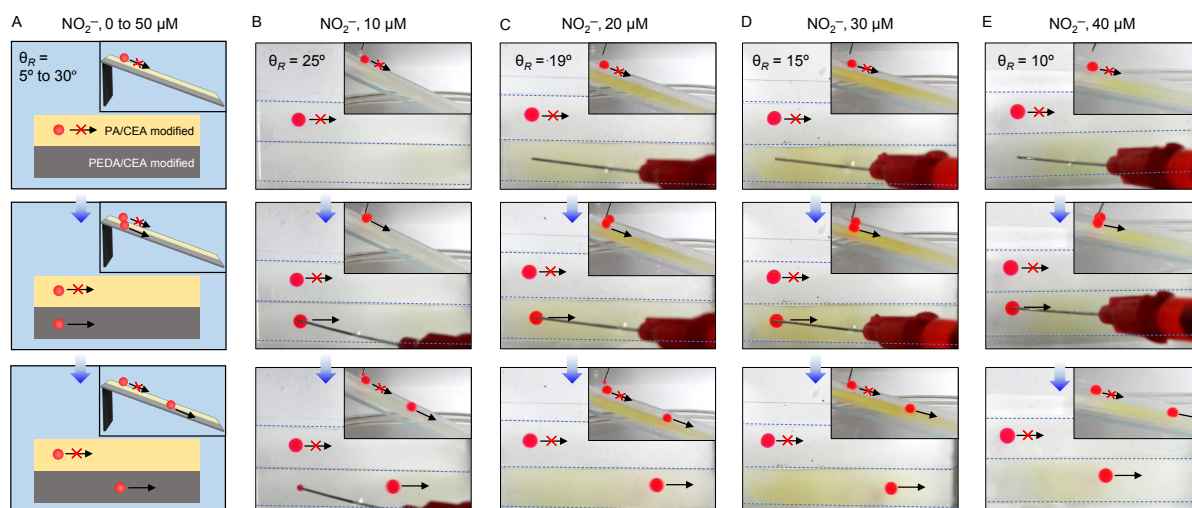


Fig. S7. A) Schematic illustration of two dual-functionalized interfaces- PA/CEA and PEDA/CEA placed alongside on a tilting surface, where beaded oil droplet adheres on the PA/CEA modified coating irrespective of the tilting angle, while the beaded oil droplet rolled-off on the PEDA/CEA modified coating, at different tilting angles as a function of nitrite ion concentration in the modified Griess reaction. The inset schematic shows the side view of the setup. B-E) Sequential photographs show the oil droplet mobility on PA/CEA and PEDA/CEA placed alongside on a tilting surface after exposure to Griess reagents as a function of different nitrite ions concentrations, where beaded oil droplet adheres on the PA/CEA modified coating irrespective of the tilting angle, while the beaded oil droplet rolled off on the PEDA/CEA modified coating, at different tilting angles as a function of nitrite ion concentration. The volume of the beaded oil droplets was 5 μL .

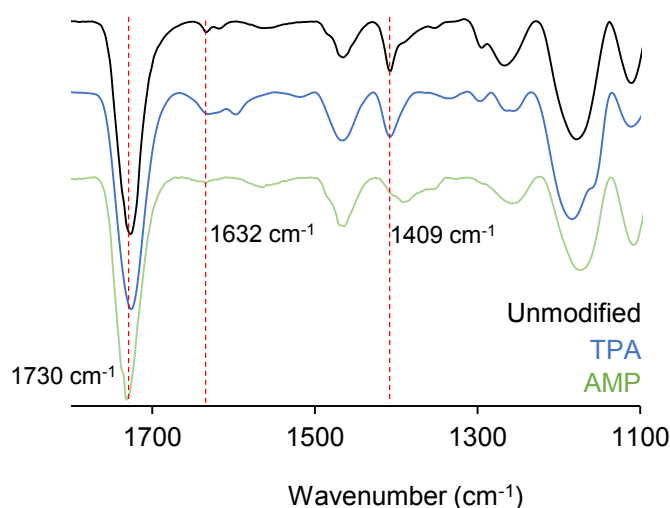


Fig. S8. Attenuated total reflection-Fourier transform infrared (ATR-FTIR) spectra of the multilayer coatings before (black) and after chemical modifications with TPA (blue) and AMP (green).

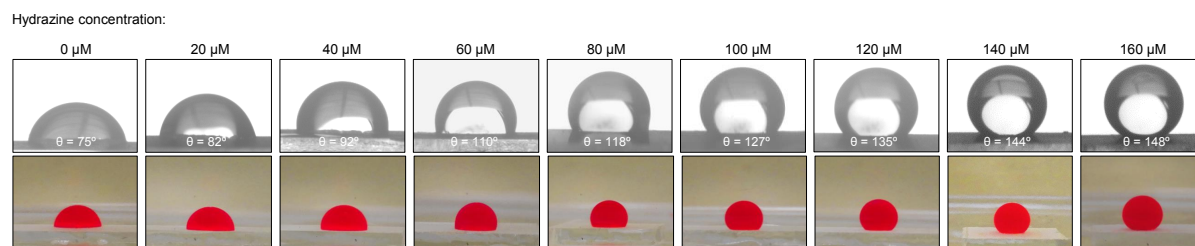


Fig. S9. Contact angle goniometer images and photographs show the effect of the concentration of hydrazine on the static contact angle of oil droplets on TPA-modified multilayer coatings after the condensation reaction of the residual aldehydes on the coating with the hydrazine.

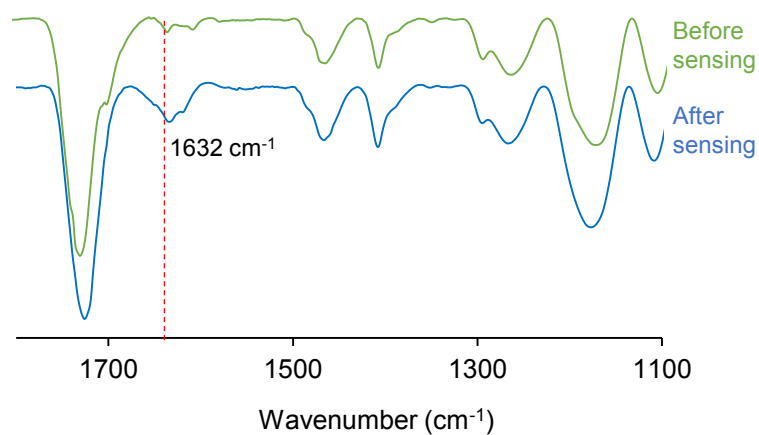


Fig. S10. ATR-FTIR spectra representing TPA-modified coating before and after modifications with hydrazine.

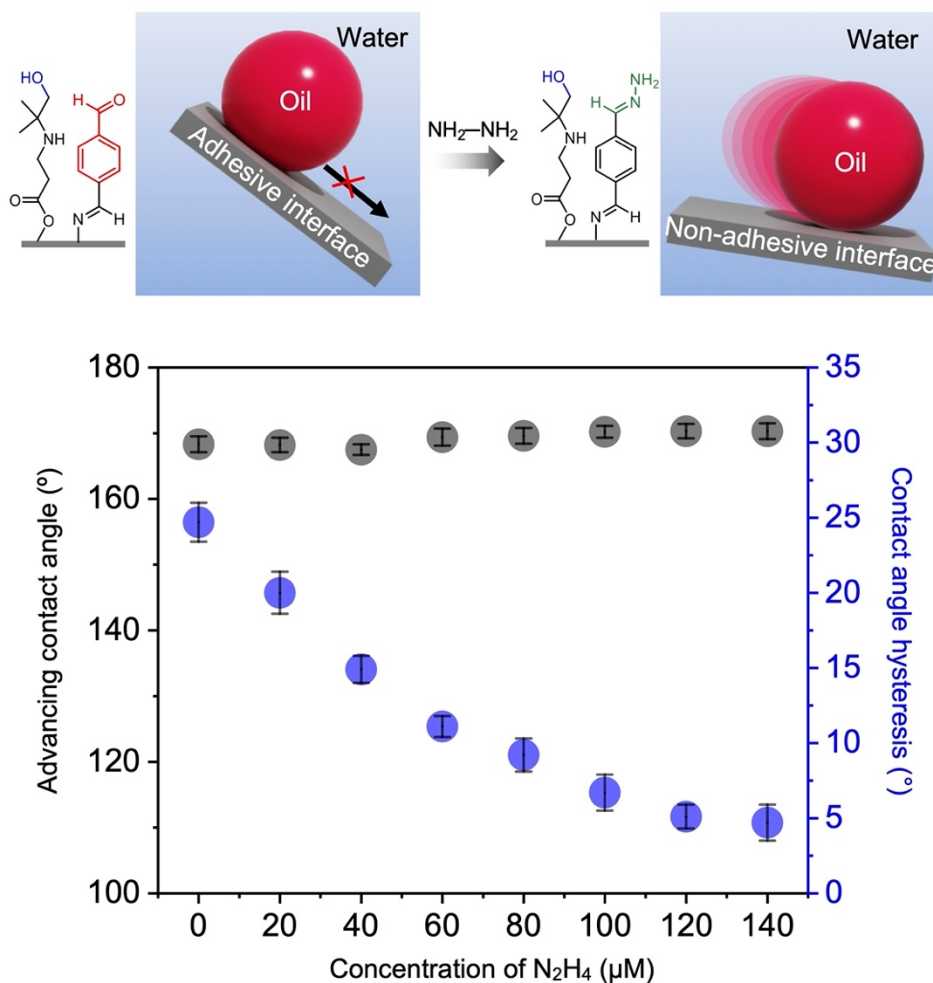


Fig. S11. Schematic depicting the dual (TPA/AMP)-functionalized multilayer coating exhibiting underwater adhesive superoleophobicity and its conversion into non- adhesive superoleophobicity on exposure to an aqueous solution of hydrazine. The plot accounting the effect of concentration of hydrazine on the advancing OCA and CAH of oil droplets on TPA/AMP-modified coatings after treatment with an aqueous solution of hydrazine.

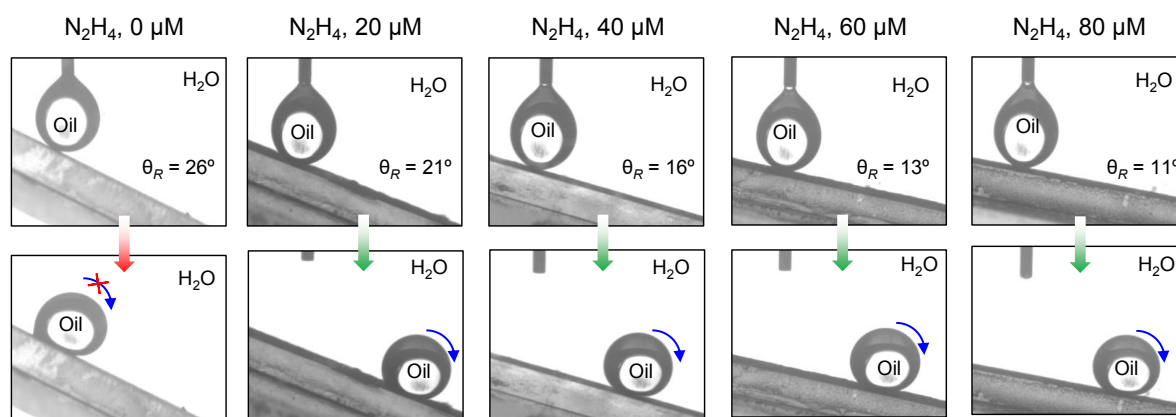


Fig. S12. Photographs showing the mobility of oil droplets on TPA/AMP-modified coating as a function of hydrazine concentration at a minimum tilting angle where the oil droplets started rolling off. The volume of the beaded oil droplets was 5 μL .

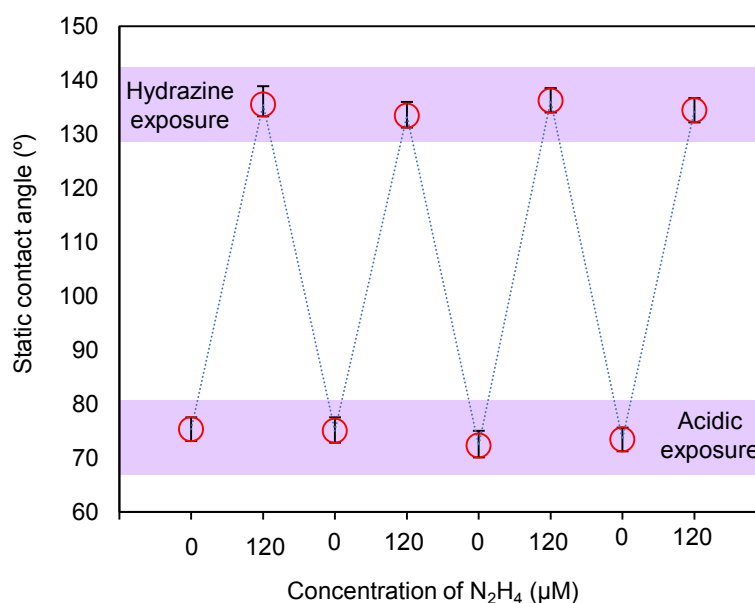


Fig. S13. Reversible manipulation of the oil contact angle on the TPA-modified surface after treatment with hydrazine, where the residual reactivity in the coating was re-installed by acidic solution treatment.